Fundamental Journals
International Journal of Fundamental Physical Sciences (IJFPS) ISSN:2231-8186
IJFPS, Vol 4, No 1, pp 01-07, March , 2014 S.N.Hosseinimotlagh
DOI:10.14331/ijfps.2014.330060
http://dx.doi.org/10.14331/ijfps.2014.330060

Calculation of Stau-Atoms and Molecules Formation Rates for Different Common Fusion Fuels in Stau Catalyzed Fusion

S.N.Hosseinimotlagh[1]*, A.Gharaati[2], M.Ghasemi ShabanKareh[3], J.Bahmani[4]

[1]Department of Physics, Shiraz Branch, Islamic Azad University, Shiraz, Iran
hoseinimotlagh@hotmail.com

[2]Department of Physics, Payame Noor University, Shiraz, Iran
agharaaati@pnu.ac.ir

[3]Department of Physics, Imam Hossein Comprehensive University, Tehran, Iran
mohammad.ghasemi@gmail.com

[4]Department of Physics, Payame Noor University, Tehran, Iran
bahmani22@yahoo.com

(*Received Jan 2014; Published March 2014*)

ABSTRACT

Stau fusion catalyzed fusion proceeds inside the fuel mixture with a wide range of temperature considered. The purpose of this paper is to present a detailed calculation of Stau-atoms and molecules formation rates for different common fusion reactions and the obtained results are compared with each other. Because these formation rates are the most important parameters in the Stau catalyzed fusion method and values of them are directly related to energy production. Our obtained results show that, selection of fusion fuel in determination of formation rate parameter plays an important role. Also, the atom formation rate for $\tilde{\tau}p, \tilde{\tau}d, \tilde{\tau}t$ are is nearly 100 times greater than $\tilde{\tau}\,^3He$.

Keywords: Fusion, Stau, Formation rate, sleptons

DOI:10.14331/ijfps.2014.330060

INTRODUCTION

Fusion, a form of nuclear energy generated when light weight atoms fuse, is the process at work in every star´s core, releasing an enormous amount of energy. Researchers have been trying to harness fusion and reproduce it on earth in a controlled manner. If they succeed, they will provide the world a safe, sustainable, environmentally responsible and abundant source of energy. For decades, the scientific community has been pursuing nuclear fusion, yet now research has reached a critical stage, as scientists are building an experimental reactor that one day may demonstrate that fusion can be used commercially to create electrical power. The main fuels used in nuclear fusion are protium, deuterium and tritium, both heavy isotopes of hydrogen. The types of fusion are Magnetic confinement fusion, Inertial confinement fusion, Muon catalyzed fusion, fusion in the solid network (such as palladium and titanium), and bubble fusion. In the following we briefly explain these. In magnetic confinement systems, electromagnets are used to contain the plasma fuel. One of the most promising options, the tokamak device, contains the plasma in a doughnut-shaped chamber.

A powerful electric current is induced in the plasma, resulting in an increase in temperature. The plasma is also heated by auxiliary systems such as microwaves, radio waves or accelerated particles. In the process, temperatures of several hundred million degrees centigrade are achieved. In inertial confinement systems, ion beams or laser beams are used to compress a pea-sized deuterium-tritium fuel pellet to extremely high densities. When a critical point is reached, the pellet is ignited through shock wave heating. Fusion power plants using this technique would ignite fuel pellets several times per second. The resulting heat is then used to generate steam that powers electricity-generating turbines. Cold fusion is hypothetical sort of fusion reaction, which don't need large amount of incredible hot plasma to start. It can be initiated by large pressure, when atoms are so close to each other that attraction caused by strong nuclear force exceed repelling electric force thereby nuclei fuse. Cold fusion, also called Low Energy Nuclear Reactions (LENR). Some metals have a large hydrogen solubility and among them palladium is the most studied. The dissolution of the deuterium (hydrogen isotope) into palladium may be achieved using either high gas pressure or an electrochemical loading process under cathodic polarization of a palladium electrode with an alkaline electrolyte. A typical electrolysis cell with a platinum anode and a palladium cathode can be used for such a process. The generation of power and energy in excess to the energy input during the process of electrochemical loading of palladium (Pd) with deuterium (D) was first announced by (Fleischmann & Pons, 1989).

In contrast, muon-based nuclear fusion does not require such ultrahigh temperatures or superdense states/ Compared to magnetic field confinement fusion and inertial confinement fusion, muon-base nuclear fusion could allow stable nuclear fusion to be induced in a smaller facility at lower cost for a longer period of time. The issue is then how muon-based nuclear fusion can be induced. Negative muon stops in deuterium and tritium mixture to form mounic hydrogen atom ($d\mu^-$,$t\mu^-$) with smaller radius (1/207) of ordinary atomic radius. The $d\mu^-$ diffuses and converts to $t\mu^-$ by muon transfer. The $t\mu^-$ collides with D_2 molecule without any Coulomb repulsive force to resonantly form $dt\mu^-$ molecule. The d-t fusion reaction occurs in the $dt\mu^-$ molecule to produce α-particle and neutron. After the d-t fusion, muon is liberated, and repeats the same process. Muon catalysed d-t fusion is a genuine cold-fusion process. Bubble fusion is one of the possible approaches to controlled fusion. Bubble fusion, also known as sono-fusion, called “acoustic inertial confinement fusion (AICF)”, is the fusion reaction possibly occurs in a high-pressure and high-temperature process called Sono-luminescence. The inertia of a collapsing bubble wall will confine the energy in a small space, and leads to an extreme rise in both temperature and pressure, which can lead to light that can be watched with naked eyes, even possibly reach the requirement of the fusion reaction. Sono-luminescence is mainly studied during the 1990s, while the application to bubble fusion is mainly studied during the last 10 years. In this article, we calculate one of the main parameters for a new method of fusion process. This method is similar to Muon catalyzed fusion (Cripps, 1993; Harms, 2002) with the difference that instead of Muon, Stau particle ($\tilde{\tau}$) has been used as a catalyst. Stau particle as Muon has negative charge but its mass much greater than the Muon mass and in our calculations is considered about $m_{\tilde{\tau}} = 100\ (Gev/c^2)$. We have named this method the Stau catalyzed fusion or abbreviations have called SCF. In (Hamaguchi, Hatsuda, Kamimura, & Yanagida, 2012; S.N. Hosseinimotlagh, 2008) this method for pure deuterium and mixed deuterium- tritium fuel has been studied. In continued work, we first briefly introduce the Stau particle and then a brief description Stau catalyzed fusion. Finally, we calculate the atoms and molecules formation rate for Stau with $m_{\tilde{\tau}} = 100\ (Gev/c^2)$ mass for traditional fusion fuels which main objective of this article.

STAU PARTICLEDISCRIPTION

In fact, supersymmetry is one of the most interesting topics beyond the standard model. This theory involves not only problems of the standard model, but also paved the way for us to describe the density of dark matter in the universe. One of the most important models in this theory is Minmal Supersymmetric Standard Model (MSSM) model (Aitchison, 2007; Drees, Godbole, & Roy, 2004; Hamaguchi, Nojiri, & de Roeck, 2007). Various particles predicted in this model, one of them has been identified as the Stau. In fact, MSSM model is the first extension of the standard model to the supersymmetry theory. Strong interacting between the superpartners namely Gluinos and Squarks with masses less than $2.5TeV$ in the Large Hadron Collider or LHC for short is a significant discovery. Physicists at the LHC have started this project from 2008. Among the Supersymmetric particles, the lightest particle (LSP) plays the essential role and in cosmology as one of the main candidates for dark matter is considered. Lightest Supersymmetric particle is probably that a Neutralino ($\tilde{\chi}_1^0$) which escape from the detector and its effects as a missing energy E_T leaves. Another possibility for the lightest particle is Gravitino ($\tilde{G}$) that is in fact a superpartners of graviton in the standard model. Our desired model for classifying Supersymmetric particles and introduce the lightest Supersymmetric particle is minimal supergravity or abbreviated mSUGRA. In this model the lightest particle is Gravitino. Gravitino are paired in a very small sector of the MSSM with other Supersymmetric particles(Hamaguchi et al., 2007).

The next lightest Supersymmetric particle (NLSP) in this model is scalar Stauin the Staus groups which we show it with $\tilde{\tau}_{-1}$and it is significantly lighter than other sleptons. Stau's decay necessarily contains the Gravitino. Also Stau has a long lifetime due to the small sector which Gravitino are paired the MSSM with other Supersymmetric particles (Hamaguchi et al., 2007). It should be noted which the Stau group is one type particle with various mass because the Stau mass dependent to production energy and gravitino mass which itself is variable. But in this article we have done calculations for the Stau with $m_{\tilde{\tau}} = 100\ (GeV/c^2)$ mass. More study about supersymmetry and Supersymmetric particles references (Ahlers, Kersten, & Ringwald, 2006; Aitchison, 2007; Buchmuller, Hamaguchi, Ratz, & Yanagida, 2004; Buchmüller, Hamaguchi, Ratz, & Yanagida, 2004; Drees et al., 2004; Hamaguchi et al., 2007; Heckman, Shao, & Vafa, 2010; Martin, 2010; Porod, 1998; Pospelov, 2007; Pradler, 2009). The Stau lifetime's by used the decay width of Stau to Gravitino and Tau is obtained by following equation (Buchmuller et al., 2004; Buchmüller et al., 2004; Hamaguchi et al., 2012; Pradler, 2009).

$$\tau_{\tilde{\tau}_1} = \frac{1}{\Gamma_{\tilde{\tau}}^{2-body}(\tilde{\tau}_1 + \tau + \tilde{G})}$$

$$= \left[\frac{\left(m_{\tilde{\tau}}^2 - m_{\frac{3}{2}}^2 - m_{\tau}^2\right)^4}{48\pi m_{\frac{3}{2}}^2 M_p^2 m_{\tilde{\tau}}^2} \left(\frac{1}{\mathrm{h}^2 c}\right) \right]^{-1} \left[1 - \frac{4 m_{\tilde{\tau}}^2 m_{\frac{3}{2}}^2}{\left(m_{\tilde{\tau}}^2 - m_{\frac{3}{2}}^2 - m_{\tau}^2\right)^2} \right]^{-\frac{3}{2}} \quad (1)$$

Where, $m_{\tilde{\tau}}$,$m_{\frac{3}{2}}$ and m_{τ} are the mass of Stau, Gravitino and Tau particles ,respectively. Also, M_p is known as the reduced plank mass such that;

$$M_p = (8\pi G_N)^{\frac{-1}{2}} \quad (2)$$

Here G_N is the gravitational constant.

$$G_N = 6.70881 \times 10^{-39} (Gev/c^2)^{-2} \quad (3)$$

$$M_p^2 = (8\pi G_N)^{-1} = 1/hc[(2.435328254 \times 10^{18})^2] \quad (4)$$

Also $1/2c$ coefficient in the equation (1) is written for transform scale to time. Now put the values $m_{\tau} = 1.78\ (Gev/c^2)$,$m_{\tilde{\tau}} = 100 (Gev/c^2)$ and $m_{\frac{3}{2}} = 20 (Gev/c^2)$ in equation (1), Stau lifetime is equal to:

$$\tau_{\tilde{\tau}_1} = 2.776233891 \times 10^7 (sec) = 0.8803379922 (years) \quad (5)$$

Now for more description of the Stau with $m_{\tilde{\tau}} = 100\ Gev/c^2$mass refers to a method of producing it. One way to generate Stau-particle is scattering reaction between fixed target of nucleons and a Muon ($\mu + N(nucleon)$) (Hamaguchi et al., 2012).

Stau production cross section is dependent on the SUSY particle spectrum. Suppose that the production cross section of sleptons is $O(1)fb$ (Porod, 1998), and Muon energy has been fired toward the target in the lab frame is about $E_{\mu} = 100TeV$. Since almost all SUSY particles decay rapidly to Stau, therefore the Stau production cross section is $O(1)fb$. Assume " Fe " target with $O(1)Km$ length and $n_N = 5 \times 10^{24} cm^{-3}$ nucleons density, then the number of produced Stau per Muons given by,

$$n_{\tau} \approx \sigma \times n_N \times 10^3 \approx 10^{-8} \quad (6)$$

The reader should be notice that the stopping range of the Muon inside the Fe target is $O(1)Km$ for $E_{\mu} = 100TeV$ (Ahlers et al., 2006; Aitchison, 2007; Buchmuller et al., 2004; Buchmüller et al., 2004; Drees et al., 2004; Fleischmann & Pons, 1989; Hamaguchi et al., 2007; Heckman et al., 2010; Porod, 1998; Pospelov, 2007; Pradler, 2009).

Also, there are the other methods for Stau production for instance the use of linear accelerators that produce Stau by using the electron-electron collision. The details about these methods in references (Ahlers et al., 2006; Aitchison, 2007; Buchmuller et al., 2004; Buchmüller et al., 2004; Drees et al., 2004; Hamaguchi et al., 2007; Heckman et al., 2010; Martin, 2010; Porod, 1998; Pospelov, 2007; Pradler, 2009) are discussed. All these methods also need to have high energy.

STAU CATALYZED NUCLEAR FUSION

In this method, the fusion reaction with entry the Stau particle into the liquid fusion fuel (eg deuterium) with $N_{fuel} = 4.25 \times 10^{22}\ atoms/cm^3$ density occurs. During this process the Stau trapped by the Coulomb field of the atomic nucleus of fuel, leading to formatting atoms that in their orbits rather than the electron, Stau particle is located. First the Stau- atom is formed in the excited state and then transition to the ground state by a process called cascade process. In the next step the Stau- atom with other atom to form Stau-molecule and finally in this molecule nuclear fusion reaction will occur. The main reason to perform the fusion between nuclei of Stau- molecules very large mass and negatively charged of Stau particle. Because of the large mass of stau, leading to severe nuclear radius and According to Bohr's famous relationships reduce it to about some Fermi which is calculated to be continue. Also the negative charge of Stau leading to neutralize the Coulomb barrier between the nuclei of Stau-molecule which this barrier is the main factor in preventing the nucleus from approaching each other and nuclear fusion occur. Under these conditions, the distance between deuterium nuclei is become of $50fm$or less and so the probability of fusion between the fuel atoms significantly increases. Also, after the fusion event between the nucleus Stau- molecule, Stau is released and re-enter another cycle. However, there are also the probability of Stau capture by the Coulomb attraction of particles produced by nuclear reactions such as ^4He that should the values of Muon sticking probability for each particles are calculated and in fusion network are considered (Hamaguchi et al., 2012; S.N. Hosseinimotlagh, 2008). The Stau Sticking probability parameter is very important in Stau catalyzed fusion but not discussed in this paper. For example, Figure (1) show how to perform the processes in Muon catalyzed nuclear fusion for pure deuterium fuel is given (S.N. Hosseinimotlagh, 2008). For further described in Table (1) reactions of fusion is presented.

Table (1): different type of nuclear reactions in the traditional fusion methods

i	Reaction channel	$Q(MeV)$
1	$d + d \to {}^3He + n$	3.1446
2	$d + d \to t + p$	3.9015
3	$d + d \to {}^4He + \gamma$	23.0710
4	$t + d \to {}^4He + n$	17.0172
5	$t + t \to {}^4He$	10.9635
6	$p + d \to {}^3He + \gamma$	5.3148
7	$d + {}^3He \to {}^4He + p$	17.7742
8	$t + {}^3He \to {}^4He + p + n$	12.4593
9	${}^3He + {}^3He \to {}^4He + 2p$	12.4413
10	${}^3He + p \to {}^4He + e^+ + \nu_e$	12.4413
11	$p + p \to d + e^+ + \nu_e$	12.4413

For calculate the Stau-atoms and Stau-molecules formation rates, we needed to calculate the Bohr radius of the atoms in the ground state for electron and Stau.

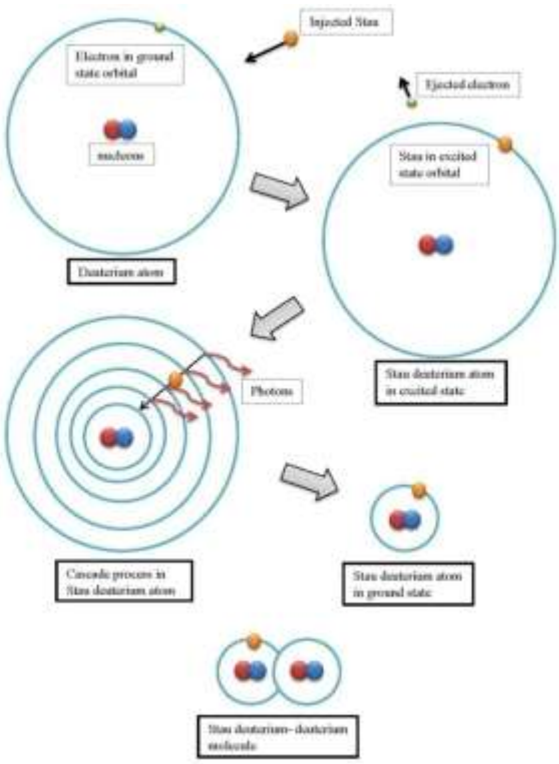

Fig.1 The Mechanism of Stau-atom and Stau-molecule formation into the pure deuterium fuel in Stau catalyzed fusion

Bohr radius and Bohr energy of atoms in ground state for hydrogen isotopes by using below relationship are calculated.

$$E_B = \frac{M}{8n^2}\left(\frac{e^2}{\varepsilon_0 hc}\right)^2 (eV) \tag{7}$$

$$a_B = \frac{e}{8\pi\varepsilon_0 E_B}(m) \tag{8}$$

In these relations, M is atomic reduce mass, n is Bohr quantum number and other parameters are physical constant. Also for radius of Stau-helium atom in ground state we used values in reference (Pospelov, 2007). The calculated values of Bohr radius and Bohr energy of different fuel atoms in ground state are presented in Table (2).

STAU ATOMIC AND MOLECULAR FORMATION RATE

In this section we calculate the atom and molecule formation rate for Stau and similarly for Muon. Formation of atoms and molecules are performed by the following reactions. In Fig.1, we see that, at first high energy Stau particle injected to a chamber of contains deuterium atoms, due to electromagnetic interactions, the electron of deuterium atom are separated from its and Stau is replaced with it ($\tilde{\tau}d$ formation mechanism in excited state). Then it in during of the cascade process with photon emission transit to the ground state. Then $\tilde{\tau}d$ in ground state collides with other deuterium atoms to formed $\tilde{\tau}dd$ molecules. As we have known, similarly, these processes also occur for the Muon catalyzed fusion. Atoms and molecules formation rates depend on the following factors:

Table 2.The calculated values of Bohr radius and Bohr energy of different fuel atoms in ground state.

	$\tilde{\tau}p$	$\tilde{\tau}d$	$\tilde{\tau}\,{}^3He$	$\tilde{\tau}t$	p	d	${}^3He$	t
$a_B(m)$	2.909×10^{-14}	1.468×10^{-14}	4.81×10^{-15}	9.895×10^{-15}	5.294×10^{-11}	5.293×10^{-11}	3.307×10^{-12}	5.292×10^{-11}
$E_B(eV)$	2.474×10^{4}	4.902×10^{4}	2.99×10^{5}	7.275×10^{4}	13.598	13.601	217.651	13.603

Energy and temperature: Formation of atoms or molecules are increased by increasing temperature and energy, since with increasing temperature the kinetic energy of the particles increases and therefore the effective collisions are increased for formation of atoms and molecules. The calculated values in tables (3) and (7) Notice.

The mass of catalyst particle: With increasing mass of catalyst particle, formation rates of atoms and molecules are reduced; because the catalyst with higher mass will be lower velocity in the fuel liquid that mean decreases the effective collision for formation Stau- atoms and molecules. For this reason, stau-atoms formation rate is different from stau-molecules. Because atoms with catalyst due to possess higher mass have lower velocity which causes to decrease effective incident with other atoms in order to molecule formation.

Scattering cross section: Increasing the scattering cross section leads to raising formation rates of atoms and molecules. For that reason the comparison table values (3) and (7) we can see that the formation rates of Stau- atoms and molecules form pure hydrogen channel (proton) more than any other channels and from pure helium is less than other channels. Since we assume a circular shape for cross section of Stau- atoms or molecules, therefore, Bohr radius of lighter atoms or molecules in ground state is more than the radius of heavier atoms or molecules. Therefore, this point leads to the increasing the cross section atoms or molecules with less mass.

Fuel density: Density of fuel particles are highly effective direct relation with the formation rates of atoms and molecules. Because with increasing fuel density of the particles, the effective collision for formation of atoms and molecules have the catalyst increases. In the following relations, we are provided the process of forming Stau-atoms and molecules.

$$\tilde{\tau} + p \xrightarrow{\lambda_a^{\tilde{\tau}p}} \tilde{\tau}p + e^-$$
$$\tilde{\tau}p + p \xrightarrow{\lambda_m^{\tilde{\tau}p-p}} \tilde{\tau}pp$$
$$\tilde{\tau}p + d \xrightarrow{\lambda_m^{\tilde{\tau}p-d}} \tilde{\tau}pd$$
$$\tilde{\tau}p + t \xrightarrow{\lambda_m^{\tilde{\tau}p-t}} \tilde{\tau}pt$$
$$\tilde{\tau}p + {}^3He \xrightarrow{\lambda_m^{\tilde{\tau}p-\,{}^3He}} \tilde{\tau}p\,{}^3He \tag{9}$$

$$\tilde{\tau} + d \xrightarrow{\lambda_a^{\tilde{\tau}d}} \tilde{\tau}d + e^-$$
$$\tilde{\tau}d + p \xrightarrow{\lambda_m^{\tilde{\tau}d-p}} \tilde{\tau}dp$$
$$\tilde{\tau}d + d \xrightarrow{\lambda_m^{\tilde{\tau}d-d}} \tilde{\tau}dd$$
$$\tilde{\tau}d + t \xrightarrow{\lambda_m^{\tilde{\tau}d-t}} \tilde{\tau}dt$$
$$\tilde{\tau}d + {}^3He \xrightarrow{\lambda_m^{\tilde{\tau}d-\,{}^3He}} \tilde{\tau}d\,{}^3He \tag{10}$$

$$\tilde{\tau} + t \xrightarrow{\lambda_a^{\tilde{\tau}t}} \tilde{\tau}t + e^-$$

$$\tilde{\tau}t + p \xrightarrow{\lambda_m^{\tilde{\tau}t-p}} \tilde{\tau}tp$$
$$\tilde{\tau}t + d \xrightarrow{\lambda_m^{\tilde{\tau}t-d}} \tilde{\tau}td$$
$$\tilde{\tau}t + t \xrightarrow{\lambda_m^{\tilde{\tau}t-t}} \tilde{\tau}tt$$
$$\tilde{\tau}t + {}^3He \xrightarrow{\lambda_m^{\tilde{\tau}t-{}^3He}} \tilde{\tau}t\,{}^3He \qquad (11)$$

$$\tilde{\tau} + {}^3He \xrightarrow{\lambda_a^{\tilde{\tau}\,{}^3He}} \tilde{\tau}p + e^-$$
$$\tilde{\tau}\,{}^3He + p \xrightarrow{\lambda_m^{\tilde{\tau}\,{}^3He-p}} \tilde{\tau}\,{}^3Hep$$
$$\tilde{\tau}\,{}^3He + d \xrightarrow{\lambda_m^{\tilde{\tau}\,{}^3He-d}} \tilde{\tau}\,{}^3Hed$$
$$\tilde{\tau}\,{}^3He + t \xrightarrow{\lambda_m^{\tilde{\tau}\,{}^3He-t}} \tilde{\tau}\,{}^3Het$$
$$\tilde{\tau}\,{}^3He + {}^3He \xrightarrow{\lambda_m^{\tilde{\tau}\,{}^3He-{}^3He}} \tilde{\tau}\,{}^3He\,{}^3He \qquad (12)$$

We show Stau-atoms and molecules formation rates for above relationship with $\lambda_{formation\ rate}$ and calculated it using the following relationship (Cripps, 1993; Harms, 2002).

$$\lambda_{formation\ rate} = N_{fuel} < \sigma v > (s^{-1}) \qquad (13)$$

Here$N_{fuel} = 4.25 \times 10^{22} atoms/cm^3$ is fuel density (e.g. deuterium, tritium and etc). Considering that the particle collisions (e.g. Stau, deuterium, and etc) to the target leads to the production of catalytic atoms and molecules at different temperatures, this issue become the cause of having different speeds in all possible directions, therefore Lambda is dependent on average of σv. Here $< \sigma v >$ is defined as follow (Angulo et al., 1999; Cripps, 1993; Fowler, Caughlan, & Zimmerman, 1967; Harms, 2002).

$$< \sigma v > = \frac{(8/\pi)^{\frac{1}{2}}}{M^{\frac{1}{2}}(KT)^{\frac{3}{3}}} \int_0^\infty \sigma E \exp(-E/_{KT})\, dE \quad (m^3/s) \qquad (14)$$

Then

$$\lambda_{formation\ rate} = N_a \frac{(8/\pi)^{\frac{1}{2}}}{M^{\frac{1}{2}}(KT)^{\frac{3}{3}}} \int_0^\infty \sigma E \exp(-E/_{KT})\, dE \qquad (15)$$

Here, σ is scattering cross section on target. M, represents the reduced mass of the system and T is the temperature. Notice that K is the Boltzmann constant Stefan. For forming of Stau-atoms, first, we assume that the atoms in the electronic ground state and with circular cross section. In this state the circular radius cross section for these atoms are the electron Bohr radius in the ground state. So to calculate the formation rate of these atoms we use the following relation (Cripps, 1993).

$$\sigma \cong \pi a^2_{B(electron)} \qquad (16)$$

In order to determine formation of Stau-molecules we use the same equation, except that the electron Bohr radius is exchanged by Stau. So for calculating the formation rate of these molecules we use the following relation (Cripps, 1993).

$$\sigma \cong \pi a^2_{B(Stau)} \qquad (17)$$

In Table (2), Bohr radius is presented for each atom that is introduced in the previous section. The calculated values of formation rates of Stau-atoms and molecules in the temperature range 20 to 1300 K in Tables (3) to (7) are presented.

Table 3. Calculated values of Stau- atoms formation rates

$T(K)$	***Atom Formation rate*** (sec^{-1})			
	$\lambda_a^{\tilde{\tau}p}$	$\lambda_a^{\tilde{\tau}d}$	$\lambda_a^{\tilde{\tau}t}$	$\lambda_a^{\tilde{\tau}\,{}^3He}$
20	2.4382×10^{11}	1.7315×10^{11}	1.4210×10^{11}	5.5509×10^{8}
300	9.4431×10^{11}	6.7062×10^{11}	5.5035×10^{11}	2.1498×10^{9}
350	1.0200×10^{12}	7.2436×10^{11}	5.9445×10^{11}	2.3221×10^{9}
400	1.0904×10^{12}	7.7437×10^{11}	6.3550×10^{11}	2.4824×10^{9}
450	1.1565×10^{12}	8.2134×10^{11}	6.7405×10^{11}	2.6330×10^{9}
500	1.2191×10^{12}	8.6577×10^{11}	7.1051×10^{11}	2.7754×10^{9}
550	1.2786×10^{12}	9.0803×10^{11}	7.4519×10^{11}	3.3992×10^{9}
600	1.3355×10^{12}	9.4841×10^{11}	7.7832×10^{11}	3.0403×10^{9}
650	1.3900×10^{12}	9.8713×10^{11}	8.1010×10^{11}	3.1645×10^{9}
700	1.4425×10^{12}	1.0244×10^{12}	8.4068×10^{11}	3.2839×10^{9}
750	1.4931×10^{12}	1.0603×10^{12}	8.7019×10^{11}	3.3992×10^{9}
800	1.5420×10^{12}	1.0951×10^{12}	8.9873×10^{11}	3.5107×10^{9}
850	1.5895×10^{12}	1.1288×10^{12}	9.2639×10^{11}	3.6187×10^{9}
900	1.6356×10^{12}	1.1615×10^{12}	9.5325×10^{11}	3.7236×10^{9}
950	1.6804×10^{12}	1.1934×10^{12}	9.7937×10^{11}	3.8257×10^{9}
1000	1.7241×10^{12}	1.2244×10^{12}	1.0048×10^{12}	3.9250×10^{9}
1050	1.7666×10^{12}	1.2546×10^{12}	1.0296×10^{12}	4.0220×10^{9}
1100	1.8082×10^{12}	1.2841×10^{12}	1.0538×10^{12}	4.1166×10^{9}
1150	1.8489×10^{12}	1.3130×10^{12}	1.0775×10^{12}	4.2091×10^{9}
1200	1.8886×10^{12}	1.3412×10^{12}	1.1007×10^{12}	4.2997×10^{9}
1250	1.9276×10^{12}	1.3689×10^{12}	1.1234×10^{12}	4.3883×10^{9}
1300	1.9657×10^{12}	1.1457×10^{12}	1.1457×10^{12}	4.4752×10^{9}

Table 4. Calculated values of Stau-atoms formation rates from$\tilde{\tau}p$ atom channel

$T(K)$	*Molecule Formation rate* (sec^{-1})			
	$\lambda_m^{\tilde{\tau}p-p}$	$\lambda_m^{\tilde{\tau}p-d}$	$\lambda_m^{\tilde{\tau}p-t}$	$\lambda_m^{\tilde{\tau}p-{}^3He}$
20	7.3599×10^{4}	5.2294×10^{4}	4.2922×10^{4}	4.2922×10^{4}
300	2.8505×10^{5}	2.0253×10^{5}	1.6624×10^{5}	1.6624×10^{5}
350	3.0789×10^{5}	2.1876×10^{5}	1.7955×10^{5}	1.7956×10^{5}
400	3.2914×10^{5}	2.3387×10^{5}	1.9195×10^{5}	1.9195×10^{5}
450	3.4911×10^{5}	2.4805×10^{5}	2.0360×10^{5}	2.0360×10^{5}
500	3.6799×10^{5}	2.6147×10^{5}	2.1461×10^{5}	2.1461×10^{5}
550	3.8596×10^{5}	4.1342×10^{5}	2.2508×10^{5}	2.2508×10^{5}
600	4.0312×10^{5}	2.8643×10^{5}	2.3509×10^{5}	2.3509×10^{5}
650	4.1958×10^{5}	2.9812×10^{5}	2.4469×10^{5}	2.4469×10^{5}
700	4.3542×10^{5}	3.0938×10^{5}	2.5393×10^{5}	2.5393×10^{5}
750	4.5070×10^{5}	3.2024×10^{5}	2.6284×10^{5}	2.6284×10^{5}
800	4.6548×10^{5}	3.3074×10^{5}	2.7146×10^{5}	2.7146×10^{5}
850	4.7981×10^{5}	3.4092×10^{5}	2.7982×10^{5}	2.7982×10^{5}
900	4.9372×10^{5}	3.5080×10^{5}	2.8793×10^{5}	2.8793×10^{5}
950	5.0725×10^{5}	3.6041×10^{5}	2.9582×10^{5}	2.9582×10^{5}
1000	5.2042×10^{5}	3.6978×10^{5}	3.0350×10^{5}	3.0350×10^{5}
1050	5.3328×10^{5}	3.7891×10^{5}	3.1100×10^{5}	3.1100×10^{5}
1100	5.4582×10^{5}	3.8782×10^{5}	3.1832×10^{5}	3.1832×10^{5}
1150	5.5809×10^{5}	3.9654×10^{5}	3.2547×10^{5}	3.2547×10^{5}
1200	5.7010×10^{5}	4.0507×10^{5}	3.3247×10^{5}	3.3247×10^{5}
1250	5.8185×10^{5}	4.1342×10^{5}	3.3933×10^{5}	3.3933×10^{5}
1300	5.9337×10^{5}	4.2161×10^{5}	3.4605×10^{5}	3.4605×10^{5}

Table 5. Calculated values of Stau-atoms formation rates from $\tilde{\tau}d$ atom channel

$T(K)$	***Molecule Formation rate*** (sec^{-1})

	$\lambda_m^{\tilde{\tau}d-p}$	$\lambda_m^{\tilde{\tau}d-d}$	$\lambda_m^{\tilde{\tau}d-t}$	$\lambda_m^{\tilde{\tau}d-\,^3He}$
20	1.8761×10^4	1.3330×10^4	1.0940×10^3	1.7923×10^3
300	7.2661×10^4	5.1625×10^4	4.2371×10^4	6.9414×10^3
350	7.8482×10^4	5.5762×10^4	4.5766×10^4	7.4975×10^3
400	8.3901×10^4	5.9612×10^4	4.8926×10^4	8.0152×10^3
450	8.8991×10^4	6.3228×10^4	5.1894×10^4	8.5014×10^3
500	9.3805×10^4	6.6648×10^4	5.4701×10^4	8.9613×10^3
550	9.8383×10^4	6.9901×10^4	5.7371×10^4	9.3987×10^3
600	1.0276×10^5	7.3009×10^4	5.9922×10^4	9.8166×10^3
650	1.0695×10^5	7.5990×10^4	6.2369×10^4	1.0217×10^4
700	1.1099×10^5	7.8859×10^4	6.4723×10^4	1.0603×10^4
750	1.1489×10^5	8.1627×10^4	6.6995×10^4	1.0975×10^4
800	1.1865×10^5	8.4304×10^4	6.9192×10^4	1.1335×10^4
850	1.2231×10^5	8.6898×10^4	7.1321×10^4	1.1684×10^4
900	1.2585×10^5	8.9418×10^4	7.3389×10^4	1.2023×10^4
950	1.2930×10^5	9.1868×10^4	7.5400×10^4	1.2352×10^4
1000	1.3266×10^5	9.4255×10^4	7.7359×10^4	1.2673×10^4
1050	1.3594×10^5	9.6582×10^4	7.9269×10^4	1.2986×10^4
1100	1.3913×10^5	9.8855×10^4	8.1135×10^4	1.3292×10^4
1150	1.4226×10^5	1.0108×10^5	8.2958×10^4	1.3590×10^4
1200	1.4532×10^5	1.0325×10^5	8.4742×10^4	1.3883×10^4
1250	1.4832×10^5	1.0538×10^5	8.6490×10^4	1.4169×10^4
1300	1.5125×10^5	1.0747×10^5	8.8203×10^4	1.4450×10^4

Table 6. Calculated values of Stau- atoms formation rates from$\tilde{\tau}t$ atom channel

$T(K)$	$Molecule\ Formation\ rate\ (sec^{-1})$			
	$\lambda_m^{\tilde{\tau}t-p}$	$\lambda_m^{\tilde{\tau}t-d}$	$\lambda_m^{\tilde{\tau}t-t}$	$\lambda_m^{\tilde{\tau}t-\,^3He}$
20	8.5155×10^3	6.0500×10^3	4.9653×10^3	1.9457×10^2
300	3.2980×10^4	2.3431×10^4	1.9230×10^4	7.5358×10^2
350	3.5623×10^4	2.5309×10^4	2.0771×10^4	8.1396×10^2
400	3.8082×10^4	2.7056×10^4	2.2205×10^4	8.7016×10^2
450	4.0393×10^4	2.8698×10^4	2.3552×10^4	9.2294×10^2
500	4.2578×10^4	3.0250×10^4	2.4826×10^4	9.7287×10^2
550	4.4656×10^4	3.1727×10^4	2.6038×10^4	1.0203×10^3
600	4.6641×10^4	3.3137×10^4	2.7196×10^4	1.0657×10^3
650	4.8546×10^4	3.4490×10^4	2.8306×10^4	1.1092×10^3
700	5.0378×10^4	3.5792×10^4	2.9375×10^4	1.1511×10^3
750	5.2147×10^4	3.7049×10^4	3.0406×10^4	1.1915×10^3
800	5.3857×10^4	3.8264×10^4	3.1403×10^4	1.2306×10^3
850	5.5514×10^4	3.9441×10^4	3.2369×10^4	1.2685×10^3
900	5.7124×10^4	4.0585×10^4	3.3308×10^4	1.3052×10^3
950	5.8689×10^4	4.1697×10^4	3.4221×10^4	1.3410×10^3
1000	6.0214×10^4	4.2780×10^4	3.5110×10^4	1.3758×10^3
1050	6.1701×10^4	4.3836×10^4	3.5977×10^4	1.4098×10^3
1100	6.3153×10^4	4.4868×10^4	3.6823×10^4	1.6850×10^3
1150	6.4572×10^4	4.5876×10^4	3.7651×10^4	1.4754×10^3
1200	6.5961×10^4	4.6863×10^4	3.8461×10^4	1.5072×10^3
1250	6.7321×10^4	4.7830×10^4	3.9254×10^4	1.5382×10^3
1300	6.8654×10^4	4.8777×10^4	4.0031×10^4	1.5687×10^3

Table7. Calculated values of Stau-atoms formation rates from $\tilde{\tau}\,^3He$ atom channel

$T(K)$	$Molecule\ Formation\ rate\ (sec^{-1})$			
	$\lambda_m^{\tilde{\tau}\,^3He-p}$	$\lambda_m^{\tilde{\tau}\,^3He-d}$	$\lambda_m^{\tilde{\tau}\,^3He-t}$	$\lambda_m^{\tilde{\tau}\,^3He-\,^3He}$
20	2.0120×10^3	1.9134×10^2	1.9457×10^2	1.9457×10^2
300	7.7925×10^3	7.4108×10^2	7.5358×10^2	7.5358×10^2
350	8.4168×10^3	8.0045×10^2	8.1396×10^2	8.1396×10^2
400	8.9980×10^3	8.5572×10^2	8.7016×10^2	8.7016×10^2
450	9.5438×10^3	9.0763×10^2	9.2294×10^2	9.2294×10^2
500	1.0060×10^4	9.5672×10^2	9.7287×10^2	9.7287×10^2
550	1.0551×10^4	1.0034×10^3	1.0203×10^3	1.0203×10^3
600	1.1020×10^4	1.0480×10^3	1.0657×10^3	1.0657×10^3
650	1.1470×10^4	1.0908×10^3	1.1092×10^3	1.1092×10^3
700	1.1903×10^4	1.1320×10^3	1.1511×10^3	1.1511×10^3
750	1.2321×10^4	1.1717×10^3	1.1915×10^3	1.1915×10^3
800	1.2725×10^4	1.2102×10^3	1.2306×10^3	1.2306×10^3
850	1.3117×10^4	1.2474×10^3	1.2685×10^3	1.2685×10^3
900	1.3497×10^4	1.2836×10^3	1.3052×10^3	1.3052×10^3
950	1.3867×10^4	1.3187×10^3	1.3410×10^3	1.3410×10^3
1000	1.4227×10^4	1.3530×10^3	1.3758×10^3	1.3758×10^3
1050	1.4578×10^4	1.3864×10^3	1.4098×10^3	1.4098×10^3
1100	1.4921×10^4	1.4190×10^3	1.4430×10^3	1.4430×10^3
1150	1.5257×10^4	1.4509×10^3	1.4754×10^3	1.4754×10^3
1200	1.5585×10^4	1.4821×10^3	1.5072×10^3	1.5072×10^3
1250	1.5906×10^4	1.5127×10^3	1.5382×10^3	1.5382×10^3
1300	1.6221×10^4	1.5427×10^3	1.5687×10^3	1.5687×10^3

CONCLUSION

According to the results of calculation values of Stau-atoms and molecules formation rates song provided in Tables (3) to (7), we studied on the different fusion reactions. Important note about the formation rate values which, the values of Stau-atoms and molecules formation rate for specific reaction are increased thus number of fusion occur are increased, and therefore increases the efficiency of energy production. For this reason, the selection of fusion fuel formation rate parameter plays an important role. According to Table (3), we observe that the values of Stau-atoms formation rates for the proton, deuterium and tritium is the same and is order of 11, and only for ^3He thesevalues are lower than and is order of 9. Also by viewing the values of Stau-molecules formation rates according to the Tables (4) to (7) we found that, the reactions possesses at least one reactant particles of them is proton, they are the highest values of molecular formation rate and are in the first group. After that, the reaction which at least one reactant particles are deuterium, they are the highest values of molecular formation rate and are in the second group. Similarly the reaction which are at least one reactant particles, tritium and ^3He, placed at the third and fourth group, respectively. (In fact, these results indicate that the values of Stau-atoms and molecules formation rates inversely dependence on the mass of the reactants was mentioned in the previous section). So the choice of nuclear fuel in addition to the selection the reaction with high values for energy production, should be considered values of Stau-atoms and molecules formation rates of each reaction So that can be selected fuel has more efficiently.

REFERENCES

Ahlers, M., Kersten, J., & Ringwald, A. (2006). Long-lived staus at neutrino telescopes. *Journal of Cosmology and Astroparticle Physics, 2006*(07), 005.

Aitchison, I. J. R. (2007). *Supersymmetry in particle physics: an elementary introduction*: Cambridge University Press.

Angulo, C., Arnould, M., Rayet, M., Descouvemont, P., Baye, D., Leclercq-Willain, C., . . . Rolfs, C. (1999). A compilation of charged-particle induced thermonuclear reaction rates. *Nuclear Physics A, 656*(1), 3-183.

Buchmuller, W., Hamaguchi, K., Ratz, M., & Yanagida, T. (2004). Gravitino and goldstino at colliders. *arXiv preprint hep-ph/0403203*.

Buchmüller, W., Hamaguchi, K., Ratz, M., & Yanagida, T. (2004). Supergravity at colliders. *Physics Letters B, 588*(1), 90-98.

Cripps, G. R. (1993). Interactive muon catalyzed and inertial confinement fusion.

Drees, M., Godbole, R. M., & Roy, P. (2004). *Theory and phenomenology of sparticles* (Vol. 1).

Fleischmann, M., & Pons, S. (1989). Electrochemically induced nuclear fusion of deuterium. *Journal of electroanalytical chemistry and interfacial electrochemistry, 261*(2), 301-308.

Fowler, W. A., Caughlan, G. R., & Zimmerman, B. A. (1967). Thermonuclear reaction rates. *Annual Review of Astronomy and Astrophysics, 5*, 525.

Hamaguchi, K., Hatsuda, T., Kamimura, M., & Yanagida, T. T. (2012). Stau-catalyzed dt Nuclear Fusion. *arXiv preprint arXiv:1202.2669*.

Hamaguchi, K., Nojiri, M. M., & de Roeck, A. (2007). Prospects to study a long-lived charged next lightest supersymmetric particle at the LHC. *Journal of High Energy Physics, 2007*(03), 046.

Harms, A. A. (2002). *Principles of Fusion Energy*: Allied Publishers.

Heckman, J. J., Shao, J., & Vafa, C. (2010). F-theory and the LHC: Stau Search. *Journal of High Energy Physics, 2010*(9), 1-61.

Martin, S. P. (2010). *A supersymmetry primer* (Vol. 1): World Scientific, Singapore.

Porod, W. (1998). Phenomenology of stops, sbottoms, staus and tau-sneutrino. *arXiv preprint hep-ph/9804208*.

Pospelov, M. (2007). Particle physics catalysis of thermal big bang nucleosynthesis. *Physical review letters, 98*(23), 231301.

Pradler, J. (2009). The long-lived stau as a thermal relic. *arXiv preprint arXiv:0909.3429*.

S.N. Hosseinimotlagh, R. S. (2008). Determination of Total Average Number of dd Fusion in Stau Cycle in Stau-Catalyzed dd Nuclear Fusion in Steady State Condition. *Infinite Energy*(80).